

# Parameter Identification of Coating Parameters to Improve Webbing Bending Response in Passive Safety Crash Simulations

Anurag Soni<sup>1</sup>, Stefan Schilling<sup>1</sup>, Martin Grikschat<sup>1</sup>, Srivathsa Jagalur<sup>2</sup>, Naveen Chandra<sup>2</sup>, Sagar Venkatesh<sup>2</sup>, Naganna Puttegowda<sup>2</sup>, Abhiroop Vishwanatha<sup>2</sup>, Mikael Dahlgren<sup>3</sup>

<sup>1</sup>Autoliv, North Germany

<sup>2</sup>Autoliv, India

<sup>3</sup> Autoliv, Sweden

## 1 Introduction

Seat belt is one of the main load bearing parts for restraining an occupant in a vehicle crash. Thus, accurate modelling of seat belt is important to achieve realistic interaction between belt to Anthropometric Test Devices dummy model in passive safety crash simulation. The belt modelling in the lap area is even more challenging because it also bears out-of-plane load during interaction with the pelvis, causing bending in webbing. Inadequate modelling of the bending response often results in rope-like effect in the lap belt during passive safety crash simulations, causing loss of contact area and eventually incorrect pelvis coupling. Such a behavior of belt is often observed with the application of THOR dummy in crash simulations, leading to an argument that simulations are not able to correctly predict submarining (slippage of belt over the pelvis to load the abdomen) and eventually incorrect estimation of the pelvis iliac forces and moments on the dummy [2]. Therefore, concerns are growing for improving the belt modelling. Besides other modelling aspects (e.g., mesh size, contact modelling, directional dependency of friction etc.), it is believed that including appropriate bending stiffness could improve dummy-to-belt interaction. There are several options available in LS-DYNA to model bending in webbing but the inevitable use of 2D sliping for its robustness and efficiency in the system models poses limitations.

Based on a collaborative study between Dynamore-Nordic and Autoliv [1], LS-DYNA updated the \*MAT\_SEATBELT\_(2D) which is capable of modelling coating feature like in \*MAT\_FABRIC (FORM = -14) and allows modelling 2D slipings. The coating can be visualized as an added layer of elastic-ideal-plastic material on the surface of membrane element which enables transfer of bending load. The coating is defined by Young's modulus (Ecoat), yield stress (Scoat) and thickness (Tcoat). It was demonstrated in [1] that coating feature in \*MAT\_SEATBELT\_(2D) improved belt bending behavior in simulations for several load cases. However, due to lack of webbing bending test data, values of the coating parameters were tuned to match the overall responses for the load cases. Since, the belt was interacting with highly deformable components (e.g., single layer and double layers of foam), outcomes of these load cases cannot be considered as the webbing-only responses. Therefore, it is necessary to optimize the coating parameters for bending response in an isolated webbing sample.

## 2 Objective

The objective of this paper is to identify optimized coating parameters based on static bending of webbing in physical tests and simulations. Sensitivities of these parameters were also analyzed. Finally, the performance of the belt model with the optimized coating values was demonstrated in belt-to-foam compression (single layer and double layers) as presented in [1].

## 3 Methods

### 3.1 Static Bending Test on Webbing

The static bending tests were performed on the webbing samples using a commercially available 2-point bending stiffness tester. *Figure 1 (a)* shows the test set-up. In the test, one side of a webbing sample was clamped into a fixture and movement on the other side was restricted by a fixed probe. The webbing was bent when the fixture was rotated (as depicted in *Figure 1 (b)*). Fixture rotation and force at probe were measured in the tests. The tests were conducted on the longitudinal direction of the webbing sample.

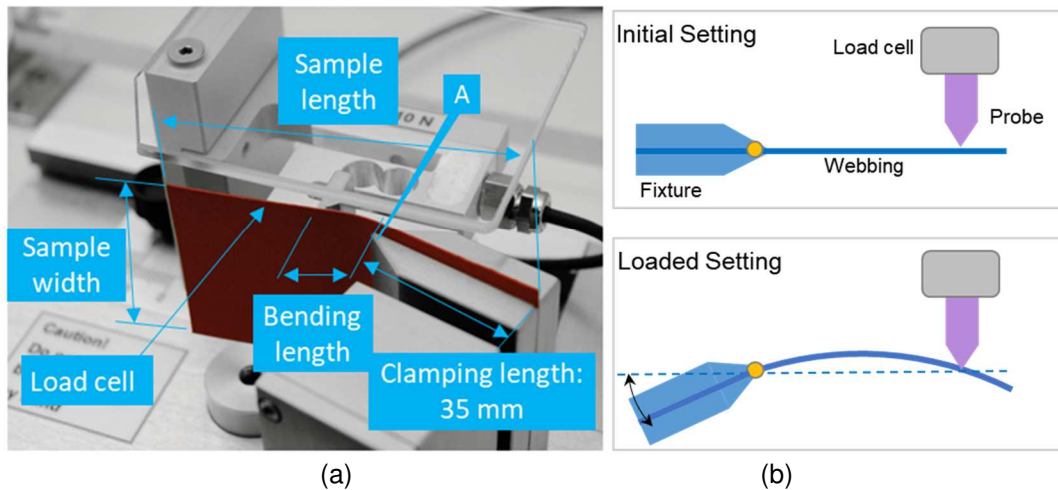


Fig.1: Bending test set-up (a) webbing specimen in the test device (b) schematic diagram illustrating bending in webbing when loaded during the test

### 3.2 Simulation Set-up and Parameter Variation

The 2-point static bending test was replicated in simulations using a simplified simulation set-up shown in Figure 2. A fixture, a probe and a piece of webbing were modelled. Their dimensions were taken from the test set-up. Considering the application for system simulations, webbing model was created with 2.5 mm element size. The fixture and the probe were modelled as rigid, and webbing was modelled deformable using \*MAT\_SEATBELT\_2D material definition. The probe was fully constrained in space whereas, the fixture could only rotate about y-axis passing through a center of rotation marked in Figure 2. The nodes on webbing mesh lying inside the fixture were constrained to fixture using tied contact definition whereas the contact between the probe and the webbing was simulated using surface-to-surface contact definition. Friction coefficient was set as 0.1 but sensitivity of friction was also investigated. A rotational displacement was applied to the fixture to achieve 90 degrees of rotation in one second duration. A force transducer was modelled to output the contact force between probe and webbing. Simulations were performed with LS-DYNA explicit solver version mpp971\_d\_R12.0.0.

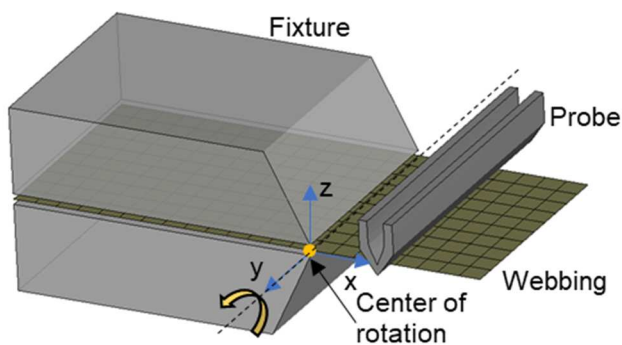


Fig.2: Simulation set-up for 2-point bending test on webbing

The coating parameters (Ecoat, Scoat and Tcoat) in matched simulations were varied. The parameter identification was performed in two stages. In the first stage, larger domain of design space was searched over and based on the simulation results, range of the parameters was narrowed down in the second stage. For the first stage, the Ecoat was varied in the range from 0.5 GPa to 4 GPa with a factor of 2. The range was set based on the elastic modulus of the webbing for the tension load. The Tcoat was varied in the range of 0.01 mm to 0.1 mm. The maximum value of the Tcoat was limited to 0.1 mm so that it remained less than 10% of the webbing physical thickness of 1.2 mm. Also, contribution of the Tcoat to membrane tension stiffness was suppressed by setting it as a negative value [3]. The Scoat was varied between 0.05 GPa to 0.4 GPa with a factor of 2. The range for Scoat was set assuming that

the yield stress (Scoat) could be about 10% of the Young's modulus (Ecoat). A full factorial parametric study was performed for the first stage. Therefore, 64 cases were simulated. *Table 1*, in appendix, lists the parameter variations. The contact force to fixture rotation from simulation was compared with the test target.

## 4 Results

### 4.1 Static Bending Tests on Webbing

In the bending tests, the force was measured only at 60 degrees of fixture rotation. This was taken as the target to match in the simulations. Therefore, to qualify for an optimum coating parameter values, it was decided that the force at 60 degrees of fixture rotation in simulation should match with the test target. In addition, it was assumed that the force should continuously increase at least till 80 degrees of fixture rotation.

### 4.2 Simulations

Effects of variation in each coating parameter on the bending response of the webbing sample are plotted in *Figure 3*. It was observed that bending in belt increased up to a certain rotation angle and further rotation did not add more bending. Consequently, in force-rotation curves force linearly rose to peak value and force level saturated to further rotation. It is evident that variations in Ecoat and Tcoat affected the bending stiffness (i.e., slope of force-rotation curves) whereas variations in Scoat affected the force level at which bending (force) saturated. For the simulated variations, it was observed that bending stiffness had a linear relation with both Ecoat and Tcoat. For a 2 folds increase in Ecoat (from 2 GPa to 4GPa) and Tcoat (from 0.025 mm to 0.05 mm), rotation to achieve the same force level reduced by half (40 degrees to 20 degrees for Ecoat and 80 degrees to 40 degrees for Tcoat).

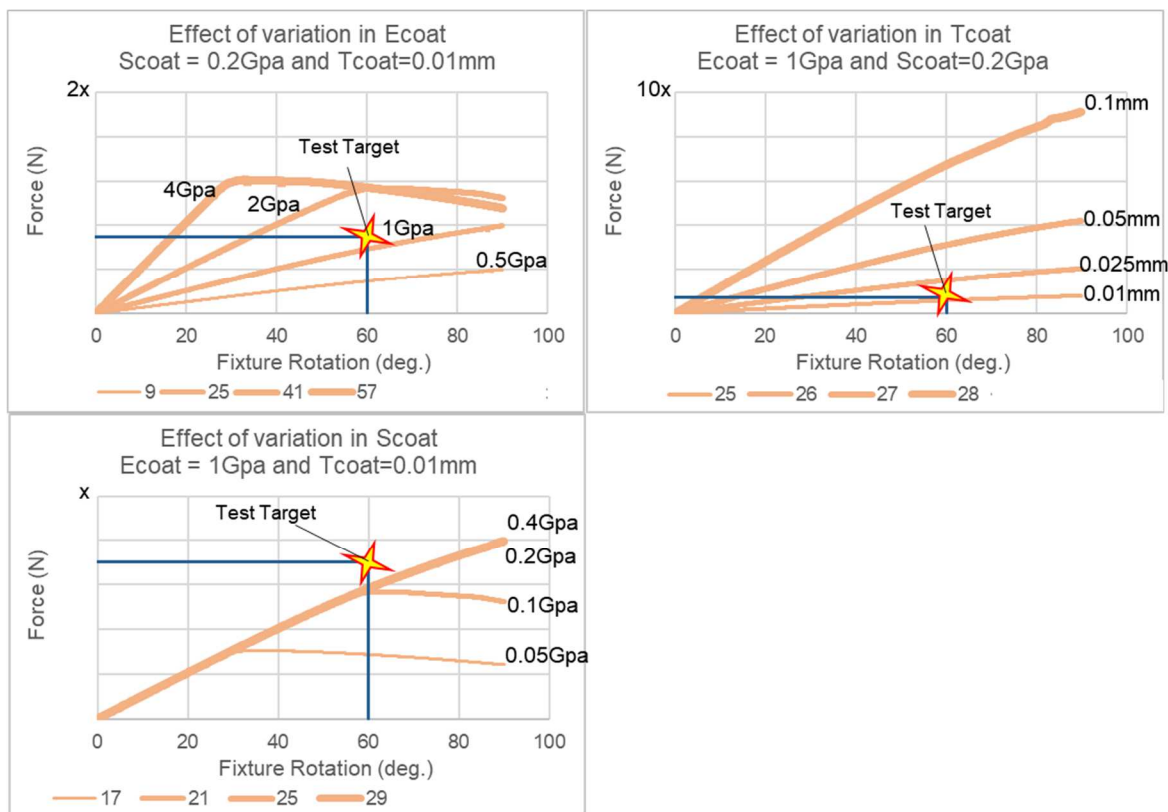


Fig.3: Force to Fixture rotation to show the sensitivity of Ecoat (top-left), Tcoat (top-right) and Scoat (bottom-left).

Force-rotation curves obtained from 64 simulations in the stage-1 of parametric study are plotted in the *Figure 4 (a)*. Comparing the test target (i.e., force level at 60 degrees rotation), 4 simulated responses (#2, #14, #25, and #29) were found to be close to the test (shown separately in *Figure 4 (b)*). From the selected cases, variation #2 was rejected because the force saturated before 80 degrees. The variation

#14 was rejected due to higher Tcoat value. Between variations #25 and #29, lower value of Scoat (i.e., 0.2 GPa) in #25 was preferred since the force did not saturate until 90 degrees of rotation. However, compared to test target, the force at 60 degrees was lower so a stage-2 of parametric study was performed with taking variation #25 as the reference for further optimization. In the stage-2 simulations, both Ecoat (1.0 GPa) and Scoat (0.20 GPa) were retained from #25 whereas Tcoat was increased from its reference value of 0.01 mm to 0.015 mm with an increment of 0.001 mm. *Figure 5* shows the force-rotation curves obtained from the stage-2 simulations. Comparing with the test target, variation #252 (Ecoat = 1GPa, Scoat = 0.2 GPa and Tcoat = 0.012 mm) was selected as an optimum.

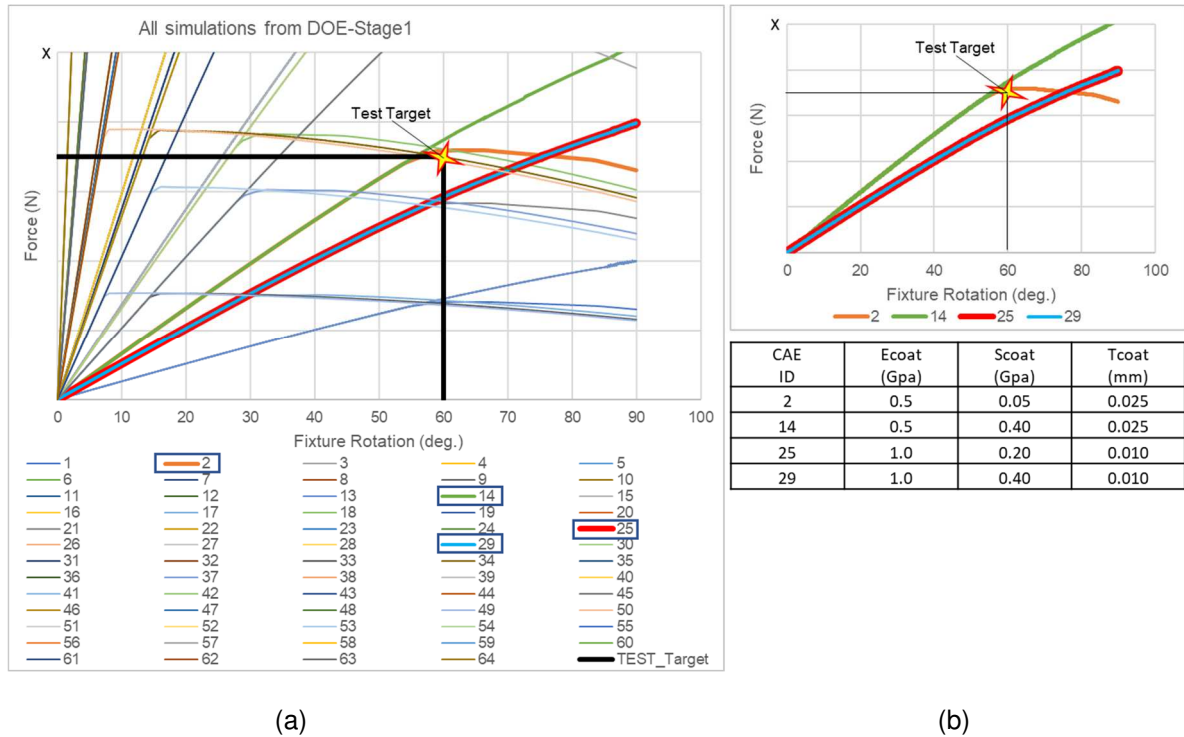


Fig.4: Force to Fixture rotation (a) plotted for all 64 cases from the stage-1 of the parametric study (b) from the selected cases which are closer to test target.

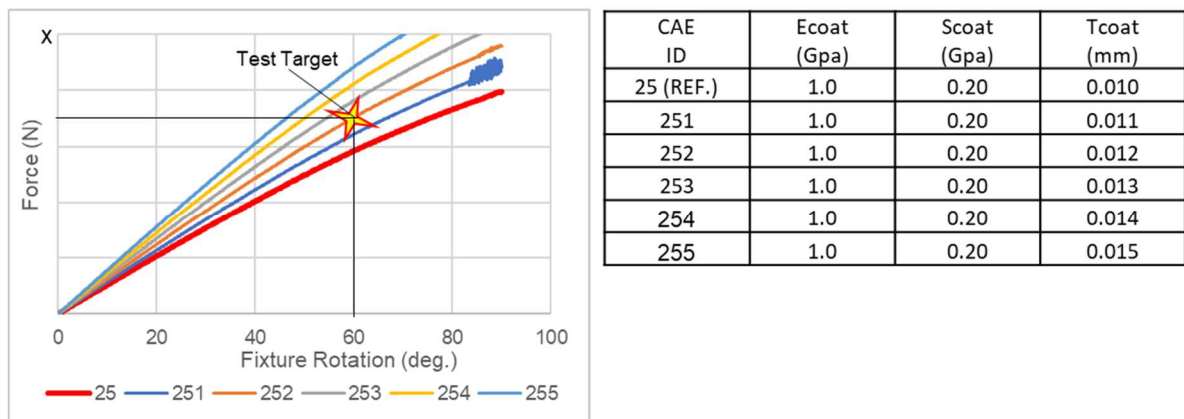


Fig.5: Force to Fixture rotation for all the cases simulated for stage-2 of the parametric study.

## 5 Performance Evaluation with Optimum Coating Parameters

### 5.1 Simulation for Webbing Bending Test

Figure 6 compares the webbing bending response for the three simulated cases: 1) coating optimized for bending in the current study, 2) without coating and 3) coating based on Dahlgren et al. (2020) [1]. It is evident that compared to the webbing response with the coating values optimized in the current

study, the webbing response with the coating values from [1] was significantly stiffer and the force saturation occurred at lower rotation (i.e., only at 19 degrees of fixture rotation). At 19 degrees of rotation, the force was about 20 times higher with coating values from [1] compared to that with the current study.

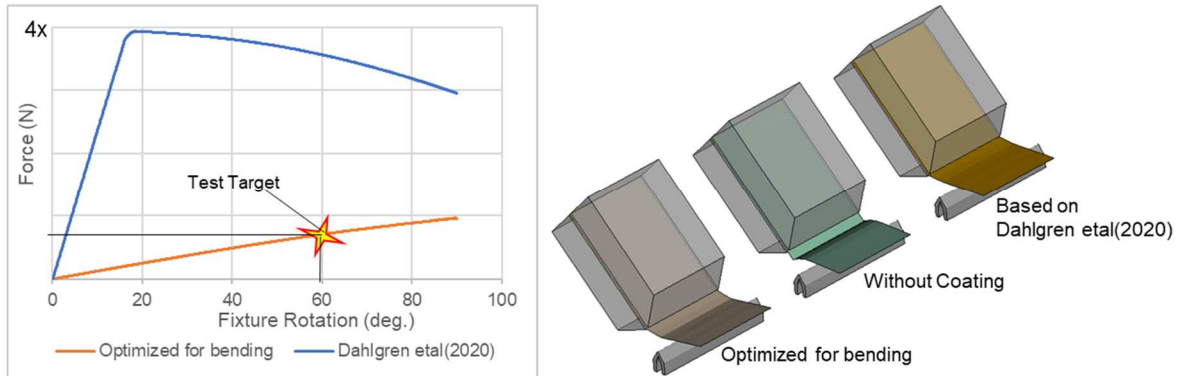


Fig.6: Force to Fixture rotation comparison between optimized coating in current study with that achieved in Dahlgren et al. (2020).

## 5.2 Belt-to-Foam Compression: Single and Double Layers of Foam

Figure 7 and Figure 8 shows the webbing deformation while compressing a single layer and double layers of foam, respectively for the two simulated cases of coating values (current study versus Dahlgren et al. (2020)) and compared it with the test at the same instance. It was observed that for the same level of compression in the foam, simulated response with the coating values from the current study was closer to the test. Particularly, the folding in the webbing at the top and the bottom edges matched closely to that observed in the test. Whereas higher bending stiffness with the coating values from Dahlgren et al. (2020) might have prevented the webbing to fold.

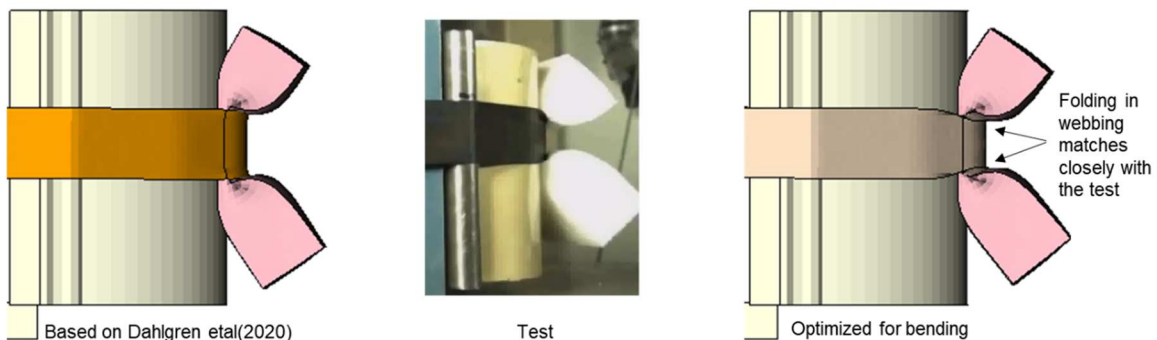


Fig.7: Belt-to-Foam Compression for single layer of Foam: Comparison between optimized coating in current study with that achieved in Dahlgren et al. (2020).

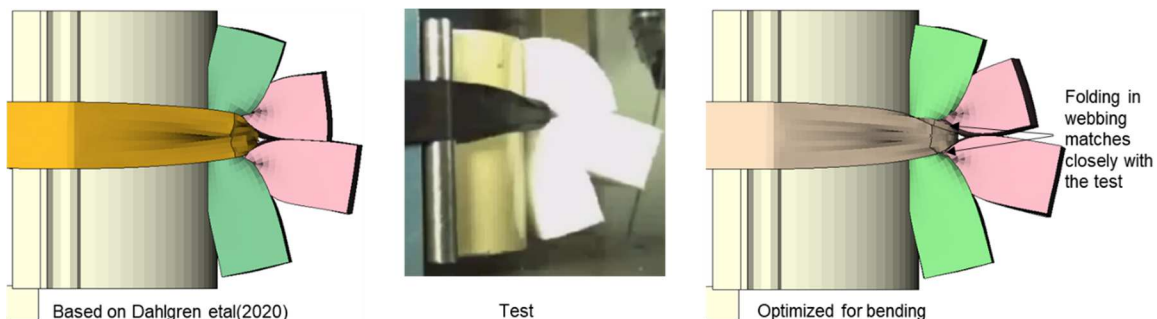


Fig.8: Belt-to-Foam Compression for double layers of Foam: Comparison between optimized coating in current study with that achieved in Dahlgren et al. (2020).

## 6 Discussion

The coating parameters (i.e., Ecoat, Scoat and Tcoat) in the \*MAT\_SEATBELT\_(2D) were optimized for seatbelt webbing material using 2-point static bending test data. For that, total 69 variations in coating

parameters, in two stages (i.e., 64 in stage-1 and 5 in stage-2), were simulated in this study. The resulting coating values showed significant improvements over the coating values achieved in [1]. It indicates the importance of optimizing the material parameters using isolated material responses instead of tuning them for an overall response. It was demonstrated that with the optimized coating parameters the belt performance improved in belt-to-foam compression simulations. Unfortunately, performance of the improved belt model could not be evaluated in the sled simulation with THOR dummy due to inconsistent requirements of solver versions for THOR (version 1.7 and 1.8) and \*MAT\_SEATBELT\_(2D). However, based on the belt response in the foam compression simulations, it is expected to improve belt-to-THOR interaction in crash simulations.

One of the limitations was that only a single data set (force at 60 degrees of fixture rotation) could be obtained from the bending tests. More data points, if not a continuous curve, were desired to capture the complete response of the webbing. This was particularly important for the larger rotation angle (above 60 degrees) to define the saturating force level and the corresponding rotation limit. It would have eventually helped in better optimizing the Scoat value which was currently selected (i.e., 0.2 GPa) based on the assumption that the force should not reach to plateau or drop before 80 degrees of fixture rotation.

It is important to highlight here that in the sled testing/simulation, the webbing often experience a complex load. There is always a certain tension force in the webbing when it undergoes in bending. The application of the tension force in the webbing was missing in the bending test setup used in the current study. The test setup could only characterize the bending response in a tension free webbing sample and hence could not replicate the real-life loading scenario. In future, a test setup needs to be devised which would be capable of applying combined loading of tension and bending in the webbing. This would facilitate in characterizing bending in webbing as a function of tension load. In view of this, \*MAT\_SEATBELT\_(2D) would also needs to be enhanced in future to consider the application of coating parameters as a function of tension force.

For further improving the webbing response in the simulations, modelling directional dependent material behavior would be important. It is well known that seatbelt is a woven fabric and thus it exhibits different mechanical properties in warp (longitudinal) and weft (transverse) directions. The current study characterized the webbing bending response in the warp direction, however, the same could not be done for the weft direction. This is because the width of serial production webbing is only 47 mm which is insufficient to be used in the existing test fixture. The size of the test fixture needs to be adapted in future to characterize bending in the weft direction and then coating parameters need to be optimized accordingly.

From the geometrical aspect it is worth mentioning that element size of the webbing mesh is also an important parameter since it controls the smallest folding length in the webbing. Therefore, the smaller the element size, the better the folding behavior but then the higher the computational cost. In a standard sled simulation, a 47 mm wide webbing is often meshed with 8 rows of elements in the width direction resulting in an element edge length of 5.875 mm. From the past experiences [1] it was realized that 18 rows of elements over width (element edge length about 2.5 mm) was a good compromise between the desired belt response and the computational cost. The optimized values in the current study are therefore limited to 2.5 mm of element size.

Sensitivity of the friction between webbing-to-probe was also studied. No significant effects on the force to fixture rotation were observed in the simulations for the friction coefficients ranged between 0.001 to 0.4 (as shown in *Figure 10 in Appendix - A*), but for higher values of friction coefficients (i.e., 0.8 and 1.0), increase in force was evident. Considering the possible range of friction coefficients (0.193 to 0.309) reported for fabric-to-metal in [4], it is believed that the choice of 0.1 for friction coefficient in the simulations for parameter optimization will not affect the selected optimum values for the coating parameters.

In addition to the material and the geometrical parameters, belt-to-dummy interaction is significantly affected by the friction definition for the contacts between the belt and the interacting dummy parts. Using directional dependent friction values (i.e., for longitudinal and transverse direction of webbing) could improve the belt slippage behavior. In future, more efforts should be applied to quantify the orthogonal friction coefficients for contact pairs between belt to dummy parts.

Although, updated \*MAT\_SEATBELT\_(2D) facilitated to model combined tension and bending response of webbing, however, it accomplished this with a double layered element approach (i.e., membrane and shell for in-plane and bending properties, respectively). In future, application of detailed contact modelling for simulating webbing-routed-through-the-buckles, instead of 2D slings, cannot be ignored. For that reason, a coupled material and element formulation to separate the bending and the tension will be needed in future to provide possibilities of more detailed modelling of the webbing.

## 7 Conclusion

The coating definition in \*MAT\_SEATBELT\_(2D) was successfully utilized for modelling the webbing bending response. It provided an additional layer of elastic-ideal-plastic material where both Ecoat and Tcoat affected the bending stiffness and Scoat controlled the force level at which bending response was saturated. The coating parameters were optimized against the webbing bending test data and thereby obtained the optimum values as 1 GPa, 0.2 GPa and 0.012 mm for Ecoat, Scoat and Tcoat, respectively. The newly optimized parameters have further developed the belt modelling compared to previous study Dahlgren et al. (2020).

## 8 Literature

- [1] Dahlgren, M., Vishwanatha, A., Soni, A., Engstrand, K., Forsberg, J., Yeh, I.,: "Belt Modelling in LS-DYNA®", 16th International LS-DYNA Conference, 2020
- [2] OSCCAR Project Deliverable D2.5 "Validation and Demonstration of Advanced Passenger Protection Principles", 2021, [www.osccarproject.eu](http://www.osccarproject.eu), (In press).
- [3] LS-DYNA Keyword User's Manual, volume II R12, Livermore Software Technology Corp., Livermore, CA, USA, 2020
- [4] Kothari, V.K., Ganga, M. K., "Assessment of frictional properties of some woven fabrics", Indian Journal of Fiber & Textile Research, Vol. 19, pp. 151-155, (1994)

## 9 Appendix - A:

CAE-ID	Ecoat (Gpa)	Scoat (Gpa)	Tcoat (mm)
1	0.5	0.05	0.01
2	0.5	0.05	0.025
3	0.5	0.05	0.05
4	0.5	0.05	0.1
5	0.5	0.1	0.01
6	0.5	0.1	0.025
7	0.5	0.1	0.05
8	0.5	0.1	0.1
9	0.5	0.2	0.01
10	0.5	0.2	0.025
11	0.5	0.2	0.05
12	0.5	0.2	0.1
13	0.5	0.4	0.01
14	0.5	0.4	0.025
15	0.5	0.4	0.05
16	0.5	0.4	0.1
17	1	0.05	0.01
18	1	0.05	0.025
19	1	0.05	0.05
20	1	0.05	0.1
21	1	0.1	0.01
22	1	0.1	0.025
23	1	0.1	0.05
24	1	0.1	0.1
25	1	0.2	0.01
26	1	0.2	0.025
27	1	0.2	0.05
28	1	0.2	0.1
29	1	0.4	0.01
30	1	0.4	0.025
31	1	0.4	0.05
32	1	0.4	0.1
33	2	0.05	0.01
34	2	0.05	0.025
35	2	0.05	0.05
36	2	0.05	0.1
37	2	0.1	0.01
38	2	0.1	0.025
39	2	0.1	0.05
40	2	0.1	0.1
41	2	0.2	0.01
42	2	0.2	0.025
43	2	0.2	0.05
44	2	0.2	0.1
45	2	0.4	0.01
46	2	0.4	0.025
47	2	0.4	0.05
48	2	0.4	0.1
49	4	0.05	0.01
50	4	0.05	0.025
51	4	0.05	0.05
52	4	0.05	0.1
53	4	0.1	0.01
54	4	0.1	0.025
55	4	0.1	0.05
56	4	0.1	0.1
57	4	0.2	0.01
58	4	0.2	0.025
59	4	0.2	0.05
60	4	0.2	0.1
61	4	0.4	0.01
62	4	0.4	0.025
63	4	0.4	0.05
64	4	0.4	0.1

Table 1: Parameter values with CAE-ID for the parametric study – Stage-1



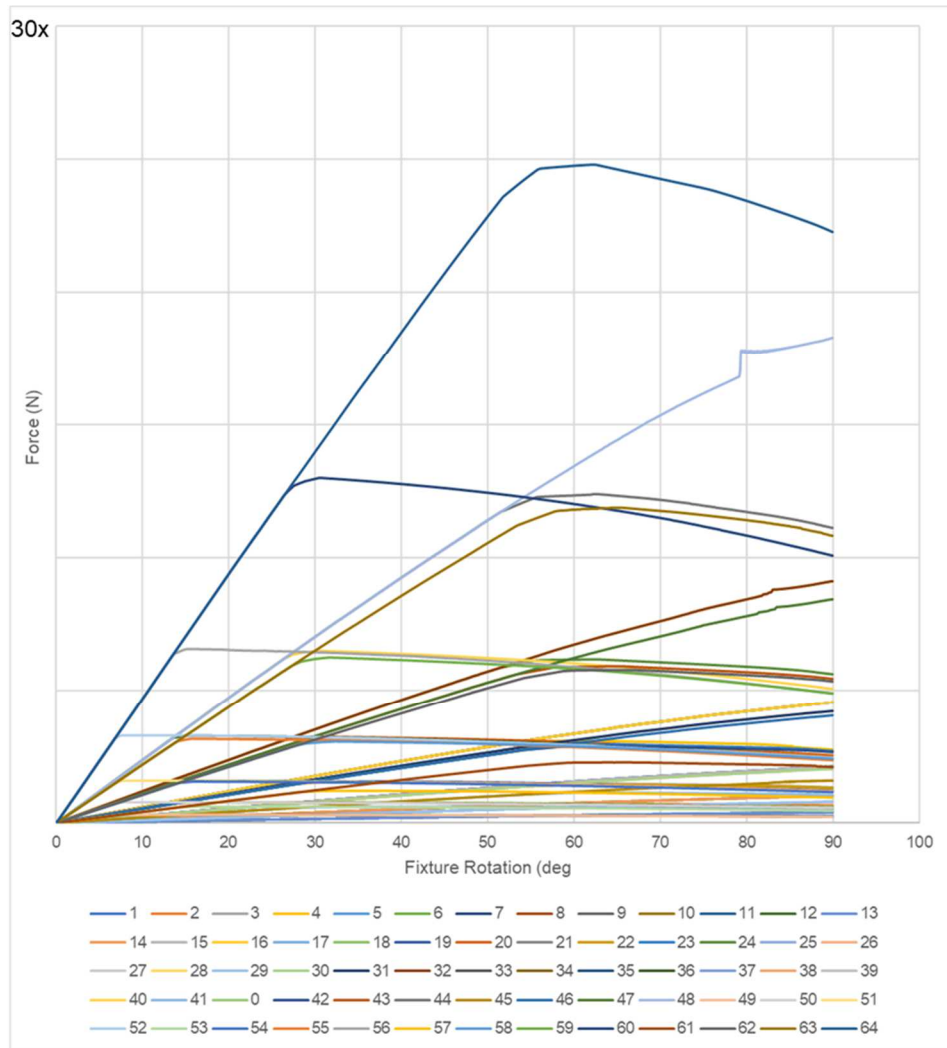


Fig.9: Force to Fixture rotation plotted for all 64 cases from the stage-1 of the parametric study

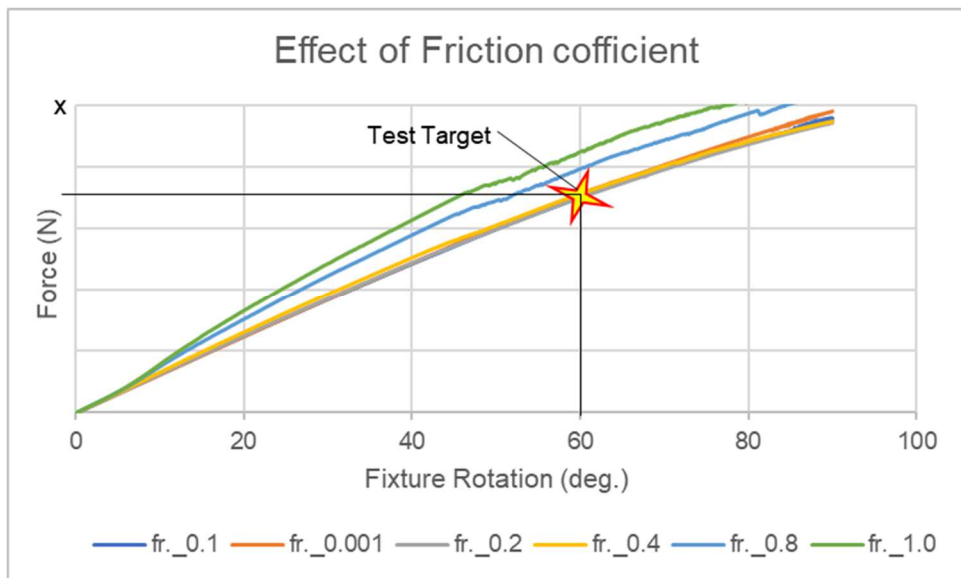


Fig.10: Force to Fixture rotation plotted for different friction coefficients (all the simulations were performed with the optimum coating values i.e.,  $E_{coat} = 0.1$  GPa,  $S_{coat} = 0.2$  GPa and  $T_{coat} = 0.012$  mm)